# Catalytic Conversion of Postconsumer PE/PP Waste into Hydrocarbons Using the FCC Process with an Equilibrium FCC Commercial Catalyst

**M.-H. Yang, Y.-H. Lin**

*Department of Chemical and Biochemical Engineering, Kao Yuan University, Taiwan 821, Kaohsiung, Republic of China*

Received 2 July 2008; accepted 8 November 2008
DOI 10.1002/app.30555
Published online 2 June 2009 in Wiley InterScience (www.interscience.wiley.com).

**ABSTRACT:** A mixture of postconsumer polyolefin waste (PE/PP) was pyrolyzed over cracking catalysts using a fluidizing reaction system similar to the fluid catalytic cracking (FCC) process operating isothermally at ambient pressure. Experiments carried out with various catalysts gave good yields of valuable hydrocarbons with differing selectivity in the final products dependent on reaction conditions. Greater product selectivity was observed with a commercial FCC equilibrium catalyst (Ecat-F1) with more than 50 wt % olefins products in the $C_3$-$C_6$ range. A kinetic model based on a lumping reaction scheme for the observed products and catalyst coking deactivations has been investigated. The model gave a good representation of experiment results. Moreover, this model provides the benefits of lumping product selectivity, in each reaction step, in relation to the performance of the FCC equilibrium catalyst used, the effect of reaction temperature, and the particle size selected.
 J Appl Polym Sci 114: 193–203, 2009

**Key words:** FCC; polymer; pyrolysis; catalyst; selectivity

## INTRODUCTION

The recycling of polymer waste is important in the conservation of resources and the environment.[1] The destruction of wastes by incineration is prevalent, but it is expensive and often generates problems with unacceptable emissions. It is also undesirable to dispose of waste plastics by landfill due to high costs and poor biodegradability. If one accepts that landfill storage is not the most rational solution and can only be considered as provisional, then one is left with the most desired primary and secondary waste recycling processes. However, these are limited to present technical limitations for the treatment of mixed polymer wastes, together with the limited size of the market for recycled products, difficulties in maintaining product quality, and fluctuations in the price. Owing to these limitations, tertiary, chemical, or feedstock recycling is growing in importance.[2] Therefore, tertiary recycling, i.e., thermal and/or catalytic conversion of waste polymers into fuels or chemicals, has been recognized as an ideal approach and could significantly reduce the net cost of disposal.[3] Two main chemical recycling routes are the thermal and catalytic degradation of waste polymers. Thermal cracking or pyrolysis is a well-known technique and is often used in petrochemical processing. The pyrolysis of waste polymers is the thermal decomposition in the absence of oxygen and is carried out in vessels, shaft kilns, autoclaves, rotary kilns, screw conveyors, or fluidized beds.[4–6] However, the thermal degradation of polymers to low molecular weight materials has a major drawback in that a very broad product range is obtained. In addition, these processes require high temperatures typically more than 500°C and even up to 900°C. These facts strongly limit their applicability and especially increase the higher cost of feedstock recycling for waste plastic treatment. Catalytic pyrolysis is being investigated as a means to address these problems.[7–9]

Catalysts can promote the degradation reaction to occur at lower temperatures, with implies lower energy consumptions. Moreover, the shape selectivity exhibited by certain catalysts allows the formation of a narrower distribution of products, which can be directed toward fuels, chemicals, and valuable hydrocarbons with higher market values. The catalytic degradation of polymeric materials has been reported for a range of model catalysts centered around the active components in a range of different catalysts, including zeolite-based such as ZSM-5, BEA, USY, MOR, and modified nanocrystalline of Y, and ZSM-5,[10–17] amorphous silica-aluminas (ASA),[18–20] and the family of mesoporous MCM materials.[21–23] However, these catalysts have been

*Correspondence to:* Y.-H. Lin (lin@cc.kyu.edu.tw).

**TABLE I**
**Catalysts Used in the Catalytic Degradation of Postconsumer Polymer Mixture**

| Catalyst | Si/Al | Surface area ($m^2/g$) | | | Pore size (nm) | Commercial name |
|---|---|---|---|---|---|---|
| | | BET[a] | Micropore | External | | |
| ZSM-5 | 17.5 | 426 | 263 | 128 | 0.55×0.51 | ZSM-5 zeolite[b] |
| USY | 13.6 | 547 | 429 | 118 | 0.74 | Ultrastabilized Y zeolite[b] |
| Ecat-F1 | 2.1 | 386 | 295 | 91 | –[c] | Equilibrium catalysts[b] |
| MCM-41 | 14.3 | 775 | 0 | 775 | 4.2 ∼ 5.2[d] | –[e] |
| ASA | 2.6 | 268 | 21 | 247 | 3.28[d] | Amorphous silica alumina[b] |

[a] Total surface area (BET).
[b] Chinese Petroleum, CPC, Taiwan, ROC.
[c] The catalyst was a mixture of zeolite with 1.3 wt % rare earth oxide (REO), a silica-alumina matrix (32.5 wt % $Al_2O_3$), and binder.
[d] Single-point BET determined.
[e] Synthesized by procedure outlined by Beck.[30]

used that even if performing well, they can be unfeasible from the point of view of practical use due to the cost of manufacturing and the high sensitivity of the process to the cost of the catalyst. An economical improvement of processing the recycling via catalytic cracking would operate in mixing the polymer waste with fluid catalytic cracking (FCC) commercial catalysts. To date, the catalyst used in the FCC process comprises 5–40% zeolite dispersed in a matrix of synthetic silica-alumina, semisynthetic clay-derived gel, or natural clay. These catalysts increase significantly the commercial potential of a recycling process based on catalytic degradation, as cracking catalysts could cope with the conversion of polymer waste co-fed into a refinery FCC unit. It is certainly possible to develop commercial processes based on these approaches.[24,25]

Unfortunately, most of studies have been used for catalytic recycling of typically pure polymer, such as linear low-density polyethylene (LLDPE), low-density polyethylene (LDPE), high-density polyethylene (HDPE), polystyrene (PS), and polypropylene (PP), over various cracking catalysts.[10–26] It seems that in the process of polymer pyrolysis, a particular kind of catalyst is effective for a particular kind of polymer. Unfortunately, it can only be applied to pure polymers and mixed polymer wastes are not recommended. A more difficult task is tertiary recycling of commingled postconsumer polymer waste because it consists of not only hydrocarbons but also nitrogen and sulfur-containing mixed polymers as well as some modified materials. Potential concepts has been investigated in our group using a laboratory catalytic fluidized bed reactor to study the product distribution and selectivity of catalytic degradation of several different textiles of postconsumer polymer wastes previously.[27–29] However, articles concerning kinetic modeling of catalytic process for polymer degradation have great limitations, which are shared with the study of other complex reaction schemes, such as catalytic cracking and reforming. An interesting approach is that of adding mixture of polymer waste into the FCC process, under suitable process conditions with the use of FCC commercial catalysts, a large number of waste polymers can be economically converted into valuable hydrocarbons. Therefore, the objective of this work is to explore the capabilities of a catalytic fluidizing pyrolysis system similar to the FCC process with the use of a FCC equilibrium catalyst (Ecat-F1) for the study of the product distribution and selectivity on the catalytic degradation of mixture of postconsumer polymer waste, and specifically for identification of suitable reaction conditions for enhancing the potential benefits of catalytic polymer recycling.

## EXPERIMENTAL

### Materials and experimental procedures

The commingled polymer waste used in this study was obtained from postconsumer plastic waste stream in South Taiwan with the component of polyethylene (∼ 64 wt % PE = ∼ 34 wt % HDPE + ∼ 30 wt % LDPE) and polypropylene (∼ 34 wt % PP) mixtures. Typically, the content of waste plastic sample tested by elemental analysis was about 85.81% C, 13.68% H, 0.17% O, 0.23% N, and 0.11% S. The catalysts used are described in Table I. All the catalysts were crushed, pelleted, and sieved to give particle sizes ranging from 75 to 180 μm. Surface area, pore volume, and pore size distribution were measured from the adsorption-desorption isotherms of nitrogen at 77 K on a Micromeritics ASAP 2020 apparatus. Total surface area of the catalysts was estimated by application of the BET equation and total pore volumes from the nitrogen adsorbed at $p/p^\circ = 0.99$ Pore size distribution was obtained following the BJH model, whereas the micropore-specific surface area and the micropore volume were calculated

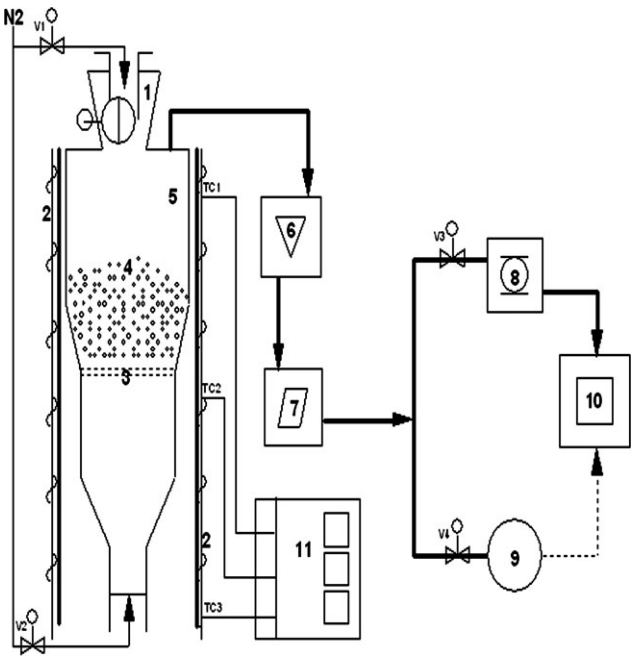


**Figure 1** Schematic diagram of a catalytic fluidized-bed reactor system: (1) Feeder, (2) Furnace, (3) Sintered distributor, (4) Fluidized catalyst, (5) Reactor, (6) Condenser, (7) Flow meter 8.16-loop automated sample system, (9) Gas bag, (10) GC, (11) Digital controller for three-zone furnace.

by the t-plot method. The external specific area used in this work was determined by the difference between the total area and the micropore area. The catalyst ($\sim$ 0.25 g) was then dried by heating in flowing nitrogen (50 mL $min^{-1}$) to 120°C at 60°C $h^{-1}$. After 2 h, the temperature was increased to 520°C at a rate of 120°C $h^{-1}$ to active the catalyst for 5 h. In contrast with the micrometer size of the crystals in conventional zeolites, ZSM-5 and USY used in this work synthesized with smaller crystallite sizes present a high proportion of external surface, which accounts for approximately 10–20% of the total zeolite surface area. High purity nitrogen was used as the fluidizing gas and the flow was controlled by a needle valve and preheated in the bottom section of the reactor tube. Before catalytic pyrolysis experiments were started, several fluidization runs were performed at ambient temperature and pressure to select: (i) suitable particle sizes (both catalyst and polymer waste) and (ii) optimize the fluidizing gas flow rates to be used in the reaction. The particle size of both catalyst (75–180 μm) and polymer (75–250 μm) were chosen to be large enough to avoid entrainment but not too large as to be inadequately fluidized. High flow rates of fluidizing stream improve catalyst-polymer mixing and external heat transfer between the hot bed and the cold catalyst. On the other hand, an excessive flow rate could cause imperfect fluidization and considerable entrainment of fines. Hence, velocities in the range 1.5 to 4 times the value of the minimum fluidation velocity of catalyst ($U_{mf}$) were used in the course of this work.

### Experimental procedures and product analysis

A process flow diagram of the experimental system is given elsewhere[9,10] and shown schematically in Figure 1. A three-zone heating furnace with digital controllers was used and the temperatures of the furnace in its upper, middle, and bottom zones were measured using three thermocouples. By these means, the temperature of the preheated nitrogen below the distributor and catalyst particles in the reaction volume could be effectively controlled to within ±1°C. The polymer feed system was designed to avoid plugging the inlet tube with melted polymer and to eliminate air in the feeder. The feed system was connected to a nitrogen supply to evacuate polymer into the fluidized catalyst bed. Thus, commingled polymer particles were purged under nitrogen into the top of the reactor and allowed to drop freely into the fluidized bed at $t = 0$ min. At sufficient polymer/catalyst ratios (more closer resembling FCC conditions) the outside of the catalyst particles are not wet with polymer, so the catalyst particles move freely.

Volatile products leaving the reactor were passed through a glass-fiber filter to capture catalyst fines, followed by an ice-acetone condenser to collect any condensable liquid product. A three-way valve was used after the condenser to route product either into a sample gas bag or to an automated sample valve system with 16 loops. The Tedlar bags, 15 L capacity, were used to collect time-averaged gaseous samples. The bags were replaced at intervals of 10 min throughout the course of reaction. The multiport sampling valve allowed frequent, rapid sampling of the product stream when required. Spot samples were collected and analyzed at various reaction times ($t$ = 1, 2, 3, 5, 8, 12, 15, 20 min). The rate ($R_{gp}$, wt % $min^{-1}$) of hydrocarbon production of gaseous products collected by automated sample system in each run was defined by the relationship:

$$R_{gp} = \text{hydrocarbon production rate of gaseous products in each spot run(g/min)} \times 100 \,/\, \text{total hydrocarbon production of gaseous products over the whole spot runs (g)}$$

Gaseous hydrocarbon products were analyzed using a gas chromatograph equipped with a thermal conductivity detector (TCD) fitted with a 1.5 m × 0.2 mm i.d. Molecular Sieve 13X packed column and a flame ionization detector (FID) fitted with a 50 m ×

0.32 mm i.d. PLOT $Al_2O_3$/KCl capillary column. A calibration cylinder containing 1% $C_1$-$C_5$ hydrocarbons was used to help identify and quantify the gaseous products. The solid remaining deposited on the catalyst after the catalytic degradation of the polymer were deemed "residues" and contained involatile products and coke. The amount and nature of the residues was determined by TGA.[26] A number of runs were repeated to check their reproducibility. It was found that the experimental error was within ±5%. Catalytic pyrolysis products ($P$) are grouped together as hydrocarbon gases ($<C_5$), liquids [gasoline ($C_5 \sim C_9$), condensate in condenser and captured in filter and BTX] and residues (coke and products, involatile at reaction temperature, deposited on catalyst) to enable the overall pyrolysis processes to be described more easily. The term "yield" as used in this artilce is defined by the relationship

$$\text{yield (wt \%)} = (P(\text{g}) \times 100)/\text{polymer fed (g)}$$

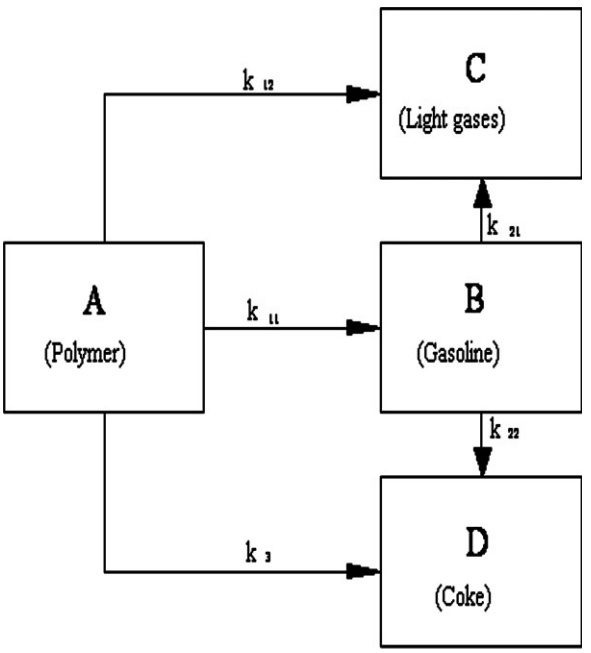


**Figure 2** Reaction scheme proposed in the four-lump model.

## Kinetic modeling

A four-lump model was proposed, which separately takes into account the unconverted feedstock, gasoline, light gases, and coke lumps and is considered to represent the product distributions. On the basis of the proposed reaction pathway shown in Figure 2, this model can be adopted for simulation of the fluidized-bed reactions. The individual rate constants are conveniently grouped as follows:

$$k_0 = k_1 + k_3 \tag{1}$$

$$k_1 = k_{11} + k_{12} \tag{2}$$

$$k_2 = k_{21} + k_{22} \tag{3}$$

where $k_0$ is the overall cracking rate constant, $k_1$ and $k_3$ are the individual disappearance rate constants from the four-lump scheme. The kinetic expression of the four-lump reaction may be written:

$$r_i\,(i = A, B, C, D) = k_i \times W_i^{n_i} \times \eta_i \tag{4}$$

where $r_i$ is the rate of consumption of the ith lump, $k_i$ is the rate constant of the ith lump, $W_i$ is the weight fraction of the ith lump, $\eta_i$ is the catalyst activity decay of the ith lump, $\eta_i$ is the reaction order and suffixes $A$, $B$, $C$, and $D$ refers to unconverted polymer, gasoline, light gases, and coke. An exponential decay function with activity decaying as function of coke on catalyst was employed.[31]

$$\eta = \exp[-\alpha C(c)] \tag{5}$$

where $C(c)$ is coke content deposited on the catalyst. It is assumed that all sites leading to the generation of unconverted polymer, gasoline, light gases, or coke are deactivated at the same rate,

$$\eta = \eta_A = \eta_B = \eta_C = \eta_D \tag{6}$$

Equation (7)–(10) were obtained with a first-order reaction and catalyst deactivation involving four simultaneous equations describing the evolution of unconverted polymer lump ($A$), the gasoline lump ($B$), the light gases lump ($C$), and the coke lump ($D$).

$$-dW_A/dt = \eta\, k_0 W_A = \eta(k_1 + k_3)W_A \tag{7}$$

$$dW_B/dt = \eta(k_{11}W_A - k_2 W_B) = \eta(k_{11}W_A - k_{21}W_B - k_{22}W_B) \tag{8}$$

$$dW_C/dt = \eta(k_{12}W_A + k_{21}W_B) \tag{9}$$

$$dW_D/dt = \eta(k_3 W_A + k_{22}W_B) \tag{10}$$

The mass balance can be written as follows

$$-dW_A/dt = dW_B/dt + dW_C/dt + dW_D/dt \tag{11}$$

Equation (7)–(11) were numerically integrated by a fourth-order Runge-Kutta algorithm for the four lumps linked with the calculation program to minimize the sum of the square deviations between the calculated and the experimental results.

**TABLE II**
**Summary of the Main products of Postconsumer Polymer Mixture (PE/PP) Degradation at Reaction Temperature of 390°C Over Various catalysts (Fluidizing $N_2$ Rate = 570 mL $min^{-1}$, Catalyst to Polymer Ratio = 20 wt % and Catalyst Particle Size = 75–120 μm)**

| | Catalyst type | | | | |
|---|---|---|---|---|---|
| Degradation results | ZSM-5 | USY | Ecat-F1 | MCM-41 | ASA |
| Yield (wt % feed) | | | | | |
| Gaseous ($\Sigma C_1 \sim C_4$) | 53.3 | 29.8 | 49.8 | 24.2 | 28.2 |
| Liquid | 36.6 | 57.6 | 38.7 | 56.7 | 55.0 |
| Gasoline ($\Sigma C_5 \sim C_9$) | 31.9 | 52.3 | 32.2 | 50.9 | 48.1 |
| Condensate liquid[a] | 3.7 | 4.1 | 4.5 | 5.3 | 4.9 |
| BTX[b] | 0.9 | 0.3 | 0.8 | 0.5 | 0.4 |
| Styrene | 0.8 | 0.9 | 1.2 | 1.7 | 1.6 |
| Residue[c] | 10.1 | 12.6 | 11.5 | 13.2 | 16.8 |
| Involatile residue | 8.5 | 8.0 | 7.9 | 11.1 | 14.4 |
| Coke | 1.6 | 4.6 | 3.6 | 2.1 | 2.4 |
| Distribution of $C_1 \sim C_9$ hydrocarbon products (wt % feed) | | | | | |
| $C_1$ | 0.2 | n.d | 0.1 | –[d] | n.d |
| $C_2$ | 0.8 | 0.1 | 0.4 | 0.1 | –[d] |
| $C_2^=$ | 3.2 | 0.7 | 1.3 | 0.2 | 0.3 |
| $C_3$ | 4.3 | 1.6 | 2.9 | 0.7 | 2.3 |
| $C_3^=$ | 15.6 | 6.6 | 16.4 | 5.2 | 6.3 |
| $C_4$ | 7.6 | 12.3 | 8.2 | 2.5 | 2.9 |
| $C_4^=$ | 21.6 | 8.5 | 20.5 | 15.5 | 16.4 |
| $C_5$ | 3.4 | 15.8 | 5.5 | 3.7 | 3.3 |
| $C_5^=$ | 8.7 | 9.3 | 9.5 | 16.7 | 14.2 |
| $C_6$ | 5.3 | 8.4 | 5.3 | 4.6 | 4.0 |
| $C_6^=$ | 6.2 | 4.3 | 6.3 | 12.3 | 11.9 |
| $C_7$ | 3.2 | 6.7 | 2.7 | 3.3 | 3.8 |
| $C_7^=$ | 3.2 | 2.6 | 1.6 | 6.7 | 6.2 |
| $C_8$ | 1.1 | 4.2 | 0.8 | 1.2 | 1.8 |
| $C_8^=$ | 0.6 | 0.8 | 0.4 | 2.2 | 2.5 |
| $\Sigma C_9$ | 0.2 | 0.2 | 0.1 | 0.2 | 0.4 |

[a] Condensate liquid: condensate in condenser and captured in filter.
[b] BTX: benzene, toluene, and xylene.
[c] Residue: coke and involatile products.
[d] less than 0.01 (wt %); n.d: not detectable.

## RESULTS AND DISCUSSION

### Degradation of commingled polymer waste (PE/PP) over various catalysts

Both the carbon number distribution of the products of polymer waste cracking at 390°C over various catalysts and the nature of the product distribution were found to vary with the catalyst used. As shown in Table II, the yield of volatile hydrocarbons for zeolitic microporous catalysts (ZSM-5 > USY) gave higher yield than zeolite-based equilibrium FCC catalyst (Ecat-F1) and nonzeolitic mesoporous catalysts (MCM-41 ≈ ASA), and the highest was obtained for ZSM-5 (nearly 90 wt %). Some similarities were observed between ZSM-5 and Ecat-F1 with $C_1$-$C_4$ and $C_5$-$C_9$ yields, which were approximately 50–53 wt % and 37–39 wt %, respectively. However, with MCM-41 and ASA the $C_1$-$C_4$ and $C_5$-$C_9$ yields were approximately 24–28 wt % and 55–57 wt %, respectively.

The bulk of the products observed with these acidic cracking catalysts were in the gaseous and liquid phase with less than 17 wt % solid residues of involatile residue and coke collected. Greater product selectivity was observed with Ecat-F1 with about 54 wt % olefins products in the $C_3$-$C_6$ range. USY produced more paraffinic streams with particularly selective to $C_5$ products generating over 25 wt % with the highest yield of i-$C_5$ (15.8 wt %). Both ASA and MCM-41 resulted in a highly olefinic product and gave rise to the broadest carbon range of $C_3$-$C_8$. The highest level of unconverted polymer was observed with ASA (16.8 wt %), whereas the highest coke yield was observed with USY (4.6 wt %). The rate of gaseous hydrocarbon evolution further highlights the slower rate of degradation over ASA and Ecat-F1 as shown in Figure 3 when comparing all catalysts under identical conditions at 390°C. The maximum rate of generation was observed after 2 min with the zeolite catalysts (ZSM-5 and USY) and MCM-41, whereas the maximum was observed after 3 min with the zeolite-based Ecat-F1 catalyst and ASA catalysts.

### Product selectivity variation with reaction conditions

The influence of operation conditions including reaction temperatures, flow rates of fluidizing gas (300–

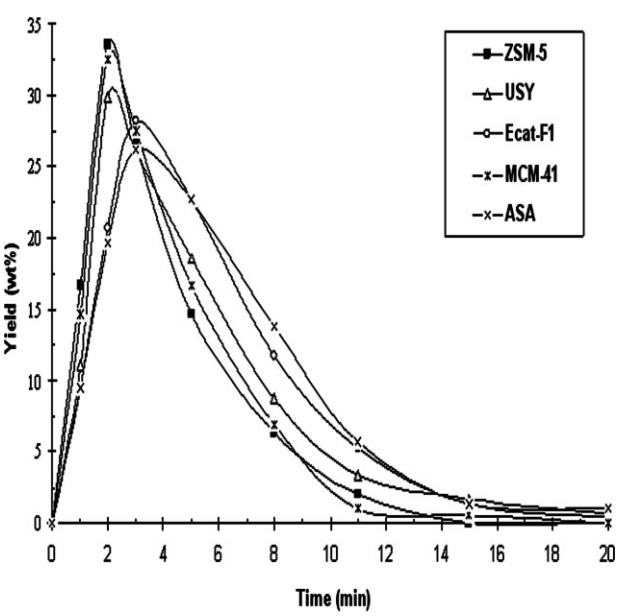


**Figure 3** Comparison of hydrocarbon yields as a function of time for the catalytic degradation of postconsumer polymer mixture (PE/PP) at 390°C over different catalysts (catalyst to polymer ratio = 20 wt %, rate of fluidization gas = 600 mL $min^{-1}$ and catalyst particle size = 75–120 μm).

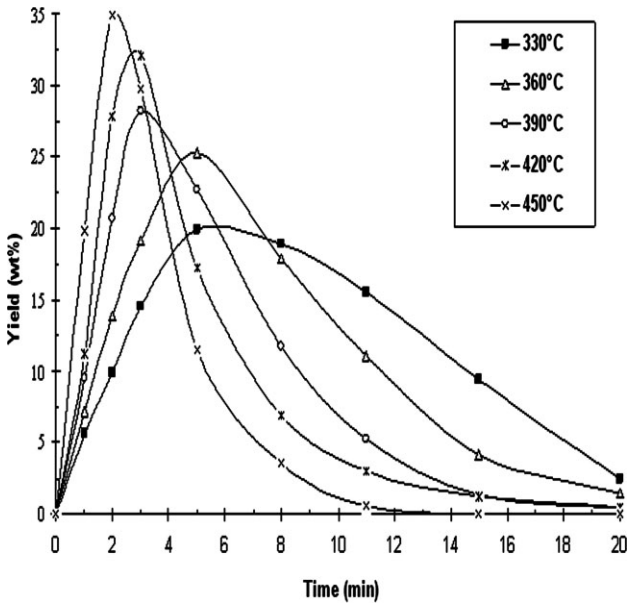


**Figure 4** Comparison of hydrocarbon yields as a function of time at different reaction temperatures for the catalytic degradation of postconsumer polymer mixture (PE/PP) over a FCC commercial catalyst (Ecat-F1) (rate of fluidization gas = 600 mL $min^{-1}$, catalyst to polymer ratio = 20 wt % and catalyst particle size = 75–120 μm).

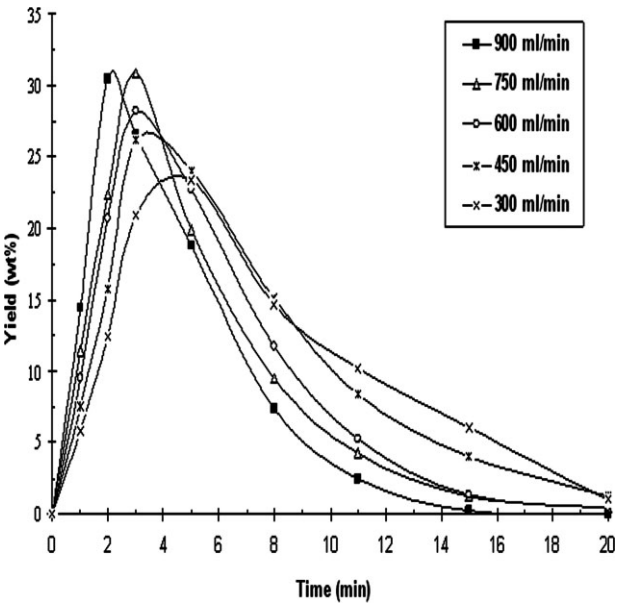


**Figure 5** Comparison of hydrocarbon yields as a function of time at different fluidization gas for the degradation of postconsumer polymer mixture (PE/PP) over an Ecat-F1 catalyst (reaction temperature = 390°C, catalyst to polymer ratio = 20 wt % and catalyst particle size = 75–120 μm).

900 mL $min^{-1}$), and catalyst type has been investigated. The rate of hydrocarbon production as a function of time at the same five temperatures is compared in Figure 4 and as expected, faster rates were observed at higher temperatures. At 450°C, the maximum rate of hydrocarbon production was 35 wt % after only 2 min with all the polymer degraded after approximately 8 min. As the temperature decreased, the initial rate of hydrocarbon production dropped and the time for the polymer to be completely degraded lengthened. At 290°C, the rate of hydrocarbon production was significantly lower throughout the whole reaction with the polymer being degraded over 20 min. The results shown in Figure 5 illustrate that for efficient polymer waste degradation good mixing is required, with a dramatic drop-off in the rate of degradation observed only at the lowest fluidizing flow used (300 ml $min^{-1}$). Furthermore, changing the fluidizing flow rate influences the product distribution. As more flow rate was increased, lower $C_1$-$C_4$ hydrocarbon gases yields but higher liquid yields and involatile products were observed. On the other hand, at low flow rates (high contact times for primary products), secondary products are observed with increased amounts of coke precursors (BTX) although the overall degradation rate is slower as shown by increasing amounts of partially depolymerized residual products (Table III).

Both acidity and diffusion constraints within individual micropores of each catalyst may play significant roles in the observed product distribution. The systematic experiments discussed in this work indicate that catalyst deactivation is being produced by active-site coverage, and consequently decrease the activity of the catalyst, giving the reason of decreasing of reaction rate with reaction time. In an attempt to estimate the change in activity of the catalyst with

**TABLE III**
**Product Distributions Shown from Ecat-F1 Catalyzed Degradation of Postconsumer Polymer Mixture (PE/PP) at Different Fluidizing $N_2$ Rates (Reaction Temperature = 390°C, Catalyst to Polymer Ratio = 20 wt %, Catalyst Particle Size = 75–120 μm and Total Time of Collection = 30 min)**

| | Fluidizing $N_2$ rates (mL/min) | | | | |
|---|---|---|---|---|---|
| Degradation results | 900 | 750 | 600 | 450 | 300 |
| Yield (wt % feed) | | | | | |
| Gaseous ($\Sigma C_1 \sim C_4$) | 46.5 | 48.2 | 49.8 | 50.4 | 51.2 |
| Liquid | 43.0 | 41.1 | 38.7 | 37.7 | 36.5 |
| Gasoline ($\Sigma C_5 \sim C_9$) | 37.4 | 35.1 | 32.2 | 30.0 | 28.3 |
| Condensate liquid[a] | 3.7 | 4.1 | 4.5 | 5.3 | 5.9 |
| BTX[b] | 0.3 | 0.5 | 0.8 | 1.4 | 1.7 |
| Styrene | 1.6 | 1.4 | 1.2 | 1.0 | 0.6 |
| Residue[c] | 10.5 | 10.7 | 11.5 | 11.9 | 12.3 |
| Involatile residue | 7.3 | 7.6 | 7.9 | 8.1 | 8.5 |
| Coke | 3.2 | 3.1 | 3.6 | 3.8 | 3.8 |

[a] Condensate liquid: condensate in condenser and captured in filter.
[b] BTX: benzene, toluene, and xylene.
[c] Residue: coke and involatile products.

increasing levels of coke related to how long can be used of the catalyst, a method using cycle of TG runs was adopted which involved the addition of fresh polymer to catalyst samples which had already been coked to different levels. In this approach, fresh polymer was added with well mixed and a further degradation run was carried out to coke catalyst. This procedure was repeated to find weight loss curves for catalyst that carried the coke from one, two or three degradation runs (Coke 1, Coke 2, Coke 3, or Coke 4). Figure 6(a) shows these results plotted together with the weight loss for fresh Ecat-F1 catalyst. Instead of deactivating the catalyst, coked catalyst was regenerated and cooled, before a further amount of polymer (equal in weight to the catalyst) was added. Figure 6(b) shows the degradation weight loss curves for fresh Ecat-F1 catalyst (Fresh) and the catalyst that had been used and regenerated between one and four times (R1 to R4). Slightly loss observed in activity was during the first regeneration, with only a few considerable losses during subsequent regeneration. It is indicates that the catalyst can regain most its initial activity on regeneration, and could be regenerated several times. In the case of catalytic degradation PE/PP waste, regeneration of the deactivated catalyst after several cycles of polymer addition can be approach, and this application for the conversion of polymer waste co-fed into a fluidizing cracking process can be practically achieved by increasing the commingled PE/PP waste to catalyst ratio. Although the benefit of the process may practically provide the great interest of using a fluidized-bed reactor for the conversion of plastic wastes, this alternative also introduces a significant limit in this type of fluidizing system in the use of polymer/catalyst ratios, which means that a high amount of catalyst must be used, mainly when compared with stirred reactor working with quite higher values. However, for the conversion of polymer waste to valuable hydrocarbons, an economical improvement of processing the recycling via catalytic cracking would operate in mixing the post-use polymer waste with commercial fluidizing cracking catalysts. Additionally, the relation in catalytic activity to catalyst deactivation was examined by the transient change in the amount of gaseous compounds produced. Rapid changes in product stream related to different degree of catalyst deactivation of both Ecat-F1 and USY was observed (Fig. 7) when the spot samples, taken during the course of the reaction, were analyzed. The deactivation varied with product selectivity is reflected in the decrease of the amount of isobutane (i-$C_4$) and isopentane (i-$C_5$) produced (product of bimolecular reaction) and the relative increase in olefins (product of monomolecular reaction), exemplified by, $C_4^=$ and $C_5^=$. The combination of 12 ring pore openings and large internal supercages of USY allow significant bimolecular reactions and yielded a saturate-rich product with a wide carbon number distribution and substantial coke levels. However, ZSM-5 is resistant to coking when coke builds up on outer surface and the product stream remains essentially unchanged, whereas the weakness and lower density of the acid sites in MCM-41 and ASA along with the increased tolerance to "coke" in the larger mesopore systems provide the most likely reasons for the lack of variation in the product stream over these catalysts. Bimolecular reactions, such as hydrogen transfer, are sterically hindered within the 10 ring channel system of ZSM-5. As expected, the zeolite-based equilibrium FCC catalyst (Ecat-F1) catalyst containing cracking activity with bimodal pore structures, which is composed of both the micropore of zeolite and the mesopore of silica-alumina used in the FCC catalyst matrix, may allow bulky reactions to occur, ultimately leading to the generation of coke and subsequently deactivation of the catalyst.

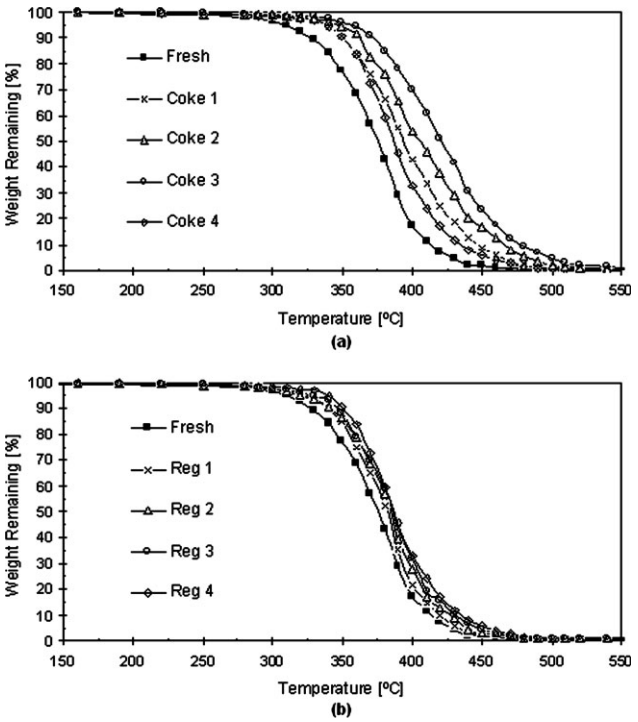


**Figure 6** Comparison of weight loss curves for postconsumer polymer mixture (PE/PP) using (a) fresh and precoked and (b) fresh and regenerated Ecat-F1 catalyst (catalyst to polymer ratio = 20 wt % and catalyst particle size = 75–120 μm).

## Kinetic results and discussion

The four lump model was used to predict product distributions for the degradation of polymers over Ecat-F1 under the operating conditions of the

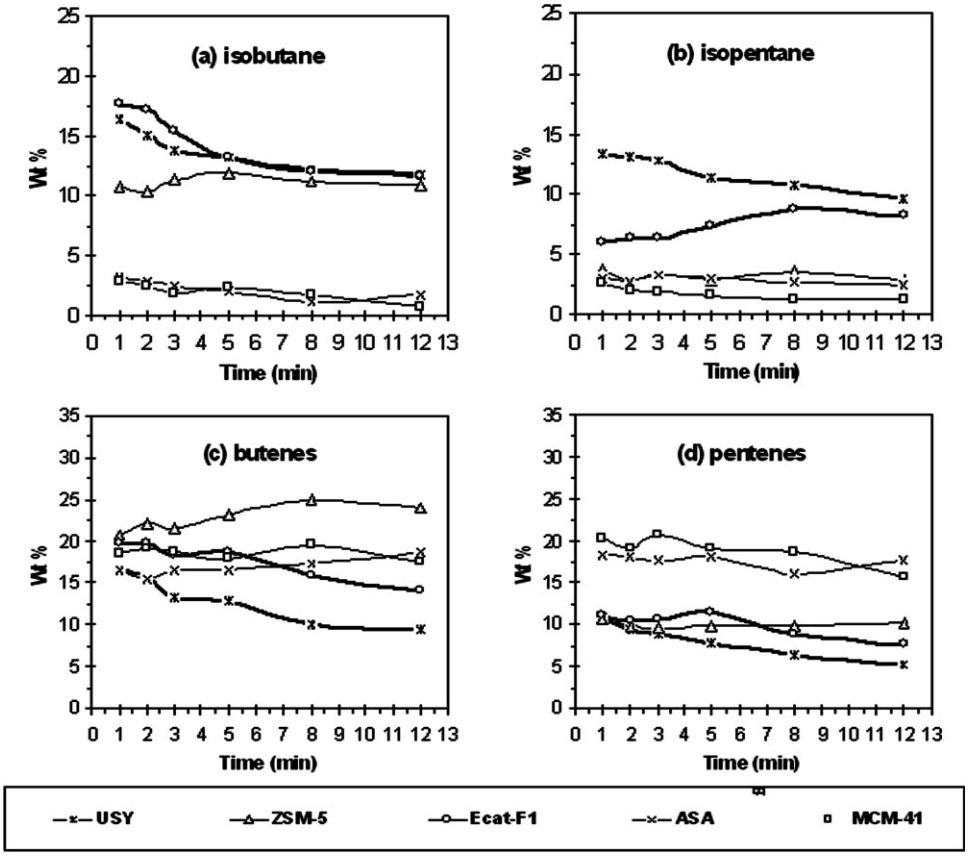


**Figure 7** Comparison of some of the main hydrocarbon products [(a) isobutane; i-$C_4$, (b) isopentane; i-$C_5$ (c) butenes, $\Sigma C_4^=$ and (d) pentenes; $\Sigma C_5^=$) as a function of time for the degradation of postconsumer polymer mixture (PE/PP) over different catalysts (reaction temperature = 390°C, catalyst to polymer ratio = 20 wt %, rate of fluidization gas = 600 mL $min^{-1}$ and catalyst particle size = 75–120 μm).

fluidized-bed reaction. As shown in Figure 8, it was found that the experimental data using various catalysts were in good agreement with the calculated values. Although $k_2 = k_{21} + k_{22}$ reflects gasoline overcracking, those two constants have in practice very different magnitudes, $k_{21} >> k_{22}$, and consequently, $k_{21}$was the only overcracking constant considered further in the analysis. The effect of different catalysts on the kinetic parameters obtained from the lumping scheme is summarized in Table IV. The lumping rate constants for each reaction step is found to be affected by the microstructure of catalysts with the larger pore size material resulting in smaller rate constants, under the same reaction conditions. The $k_{11}$ value for the catalysts used in this study was higher for zeolites (ZSM-5 and Ecat-F1) than for ASA, whereas the $k_{12}$ value for Ecat-F1 was higher than for ASA, but much lower than for ZSM-5. This suggests that the value of both $k_{11}$ and $k_{12}$ for the catalysts used in this study for the given reaction stream was dependent on the nature of the acid sites, which are much stronger in both ZSM-5 and Ecat-F1 than in ASA. Table IV also shows that the selectivity to gasoline ($k_{11}/k_0$) was similar for ASA (62.4 %) and Ecat-F1 (56.3 %), but much higher than for ZSM-5 (38.9%). ASA with large mesopores and low acidity (very small value of $k_{21}$ with less gasoline overcracking) gave rise to the broadest carbon range ($C_5$-$C_9$). A much higher selectivity to light gases ($k_{12}/k_0$) fo ZSM-5 (60.5%) compared with Ecat-F1 and ASA (40.4 % and 35.4%) was obtained, which reflects, presumably, increased cracking of pre-gasoline products to light gases with ZSM-5 as compared to the other catalysts. The difference in the value of $k_{21}$ for different catalysts is in the order ZSM-5 > Ecat-F1 > ASA. This order presumably reflects the differences in the activity of the catalyst for the cracking of molecules in the gasoline fraction. The smaller pores in ZSM-5 generate a higher concentration of smaller gasoline molecules, e.g., $C_6 \sim C_8$, which also enhances production of light gases. The relatively low values of the $k_{21}$ constant point toward only a moderate contribution to light gases by overcracking of gasoline for all the conditions studies for Ecat-F1. Both acidity and diffusion constraints within individual surface areas of each catalyst may play significant roles in the apparent rate constant and product selectivity. Because of nonvolatile

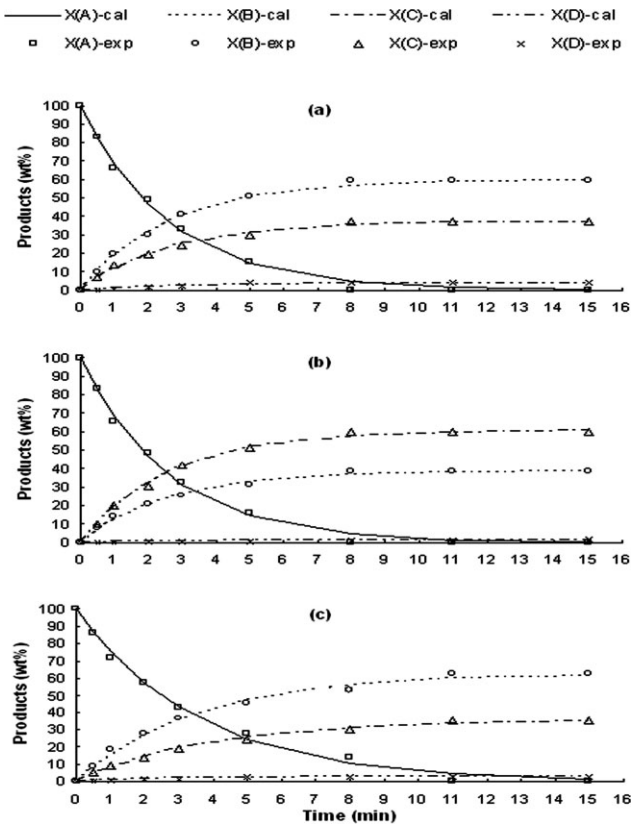


**Figure 8** Comparison of calculated (-cal) and experimental (-exp) products using the four lump model for catalytic conversion of postconsumer polymer mixture (PE/PP) over (a) Ecat-F1, (b) ZSM-5, and (c) ASA. X(A): unconverted polymer; X(B): gasoline; X(C): light gases; X(D): Coke (reaction temperature = 390°C, fluidizing $N_2$ rate = 600 mL $min^{-1}$, catalyst to polymer ratio = 20 wt % and catalyst particle size = 75–120 μm).

products with high molecular weight materials formed and consequently deposited in the catalyst system, it is difficult to take them away during the course of the reaction, and this results in some degree of increasing the yield of coke deposited on Ecat-F1 compared to ZSM-5. The Ecat-F1 catalyst containing cracking activity with bimodal pore structures, which is composed of both the micropore of zeolite and the mesopore of silica-alumina used in the FCC catalyst matrix, may allow bulky reactions to occur, ultimately leading to the generation of coke and subsequently deactivation of the catalyst. In contrast, ZSM-5 is resistant to coking when coke builds up on outer surface and the product stream remains essentially unchanged. Therefore, the deviation product yield for both Ecat-F1 and ZSM-5 catalysts could be ascribed to the nature of scission degradation in the presence of each catalyst and the differences in product selectivity from transient change in volatile fragment diffusion to the effect of different level of coke content. Moreover, the value of the $k_3/k_0$ (coke selectivity) in Ecat-F1 (3.3%) than with ASA catalyst (2.2%) may indicate possible constraints on the diffusion of liquid polymer into the pores, although the differences in the nature of the sites may also be relevant. However, ZSM-5 with narrower pore openings (0.55 × 0.51 nm) and no supercages, the bulky feed molecules have restricted access to the internal active catalytic sites and special restrictions within the pore system tend to inhibit the bimolecular processes leading to coke production (0.6%).

The rate constants for the catalytic degradation of commingled polymer waste over Ecat-F1 with particle sizes of 125–180 μm and 75–120 μm at five different temperatures (330–450°C) are listed in Table V. The selectivity toward the gasoline fraction ($k_{11}/k_0$) as a function of reaction temperature shows that the amount of gasoline formation decreased with increasing reaction temperature from 330 to 430°C then increased at 450°C. On the other hand, the results show the highest amount of light gases ($k_{12}/k_0$) occurred at 430°C rather than at the higher temperature of 450°C. It could be the case that selectivity products of light gases increased with increasing reaction temperature and gasoline decreased with an increase in temperature below 430°C. But at higher temperature (450°C), the degradation of commingled polymer waste to volatile products may proceed both by catalytic and thermal reactions leading to the variation of product distributions. The external surface of the catalysts is an important factor controlling activity and selectivity. From values of $k_{11}/k_0$ and $k_3/k_0$, the smaller particle Ecat-F1-S catalyst (75–120 μm) shows a higher selectivity for gasoline

**TABLE IV**
**Comparison of Apparent Rate Constants and Product Selectivity Using lumping Model for Postconsumer Polymer Mixture (PE/PP) Cracking Over Different Catalysts (Reaction Temperature = 390°C, fluidizing $N_2$ Rate = 600 mL $min^{-1}$, Catalyst to Polymer Ratio = 20 wt %, and Catalyst Particle Size = 75–120 μm)**

| Catalyst | $k_{11} \times 10^{-2}$ ($min^{-1}$) | $k_{12} \times 10^{-2}$ ($min^{-1}$) | $k_3 \times 10^{-2}$ ($min^{-1}$) | $k_{21} \times 10^{-2}$ ($min^{-1}$) | $k_{11}/k_0$ (%) | $k_{12}/k_0$ (%) | $k_3/k_0$ (%) |
|---|---|---|---|---|---|---|---|
| Ecat-F1 | 22.7 | 16.3 | 1.32 | 0.14 | 56.3 | 40.4 | 3.3 |
| ZSM-5 | 27.3 | 40.5 | 0.39 | 0.20 | 38.9 | 60.5 | 0.6 |
| ASA | 17.3 | 9.8 | 0.80 | 0.05 | 62.4 | 35.4 | 2.2 |

$k_0 = k_{11} + k_{12} + k_3$.

**TABLE V**
**Comparison of Product Selectivity for the Degradation of Postconsumer Polymer Mixture (PE/PP) Over Different Particle Size of Ecat-F1 Catalyst in the Temperature Range 330–450°C Using the Lumping Model (Fluidizing $N_2$ Rate = 600 mL $min^{-1}$ and Catalyst to Polymer Ratio = 20 wt %)**

| | Ecat-F1-S (75–120 μm) | | | Ecat-F1-L (125–180 μm) | | |
|---|---|---|---|---|---|---|
| Temperature (°C) | $k_{11}/k_0$ (%) | $k_{12}/k_0$ (%) | $k_3/k_0$ (%) | $k_{11}/k_0$ (%) | $k_{12}/k_0$ (%) | $k_3/k_0$ (%) |
| 330 | 66.2 | 31.5 | 2.3 | 63.5 | 33.8 | 2.7 |
| 360 | 62.1 | 35.5 | 2.4 | 58.6 | 38.5 | 2.9 |
| 390 | 59.0 | 38.3 | 2.7 | 56.3 | 40.4 | 3.3 |
| 430 | 56.5 | 40.6 | 2.9 | 54.1 | 42.7 | 3.3 |
| 450 | 62.7 | 34.3 | 3.0 | 60.3 | 36.3 | 3.4 |

$k_0 = k_{11} + k_{12} + k_3$.

(56.5–66.2% vs. 54.1–63.5%) and a lower selectivity for coke (2.3–3.0% vs. 2.7–3.4%) than the larger particle Ecat-F1-L catalyst (125–180 μm). The Ecat-F1 catalyst containing cracking activity with bimodal pore structures, which is composed of both the micropore of zeolite and the mesopore of silica-alumina used in the FCC catalyst matrix, can provide the cracking ability when they are enough accessible to the reactant and may allow bulky reactions to occur, ultimately leading to the generation of hydrocarbon products with some coke content deposited on the catalyst. The result appears that the feed can be cracked at or close to the external surface of the catalysts and therefore, the controlling catalytic parameters will be not only the total number of acid sites but also the number of accessible ones related to the particle size selected.

## CONCLUSIONS

A catalytic fluidizing reaction system has been used to obtain a range of volatile hydrocarbons by catalytic degradation of polymer waste in the temperature range 330 to 450°C. The catalytic degradation of polymer waste over a commercial FCC equilibrium catalyst (Ecat-F1) using fluidizing cracking reactions was shown to be a useful method for the production of potentially valuable hydrocarbons. Greater product selectivity was observed with Ecat-F1 with more than 50 wt % olefinic hydrocarbons in the $C_3$-$C_6$ range. Observed differences in product yields and product distributions can be influenced by the change in reaction conditions.

A kinetic model with four lumps, representing unconverted polymer, light gases, gasoline, and coke was used to determine the kinetics of catalytic degradation of the postconsumer polymer waste. A good fit between calculated and experimental results was obtained. This model provides the benefits of lumping product selectivity, in each reaction step, in relation to the performance of the FCC catalyst used, the particle size selected, and the effect of reaction temperature. It is concluded that the use of this reaction system coped with a FCC equilibrium catalyst can be a better option since it may lead to a cheaper process with valuable products and can be further used as an adequate approach for the catalytic recycling of polymer waste.

## References


1. Billingham, N. C. Polymers and the Environment, Gerald Scott; Royal Society of Chemistry: London, 1999.
2. Cornell, D. D. Plastics, Rubber, and Paper Recycling: A Pragmatic Approach; American Chemical Society: Washington, 1995; p 72.
3. Brandrup, J.; Bittner, M.; Michaeli, W.; Menges, G. Recycling and Recovery of Plastics; Carl Hanser Verlag: Munich, New York, 1996.
4. Hardman, S.; Leng, S. A.; Wilson, D. C. Eur. Pat. Appl. 567,292 (1993).
5. Kaminsky, W.; Schlesselmann, B.; Simon, C. J Anal Appl Pyrol 1995, 32, 19.
6. Sodero, S. F.; Berruti, F.; Behie, L. A. Chem Eng Sci 1996, 51, 2805.
7. Mastellone, M. L.; Perugini, F.; Ponte, M.; Arena, U. Polym Degrad Stab 2002, 76, 479.
8. Lin, Y. H.; Yang, M. H. J Anal Appl Pyrol 2008, 83, 101.
9. Lin, Y. H.; Yang, M. H.; Yeh, T. F.; Ger, M. G. Polym Degrad Stab 2004, 86, 121.
10. Lin, Y. H.; Yen, H. Y. Polym Degrad Stab 2005, 89, 101.
11. Ishihara, Y.; Nanbu, H.; Saido, K.; Ikemura, T.; Takesue, T. Bull Chem Soc Jpn 1991, 64, 3585.
12. Ohkita, H.; Nishiyama, R.; Tochihara, Y.; Mizushima, T.; Kakuta, N.; Morioka, Y.; Namiki, Y.; Katoh, H.; Sunazyka, H.; Nakayama, R.; Kuroyanagi, T. Ind Eng Chem Res 1993, 32, 3112.
13. Uemichi, Y.; Nakamura, J.; Itoh, T.; Garforth, A.; Dwyer, J. Ind Eng Chem Res 1999, 38, 385.
14. Aguado, J.; Serrano, D. P.; Escola, J. M.; Garagorri, E.; Fernandez, J. A. Polym Degrad Stab 2000, 70, 97.
15. Lee, S. Y.; Yoon, J. H.; Kim, J. R.; Park, D. W. Polym Degrad Stab 2001, 74, 297.
16. Dawood, A.; Miura, K. Polym Degrad Stab 2002, 76, 45.
17. Audisio, G.; Silvani, A.; Beltrame, P. L.; Carniti, P. Polym Degrad Stab 1989, 26, 209.
18. Gao, Z.; Ksuyoshi, K.; Amasaki, I.; Nakada, M. Polym Degrad Stab 2003, 80, 269.
19. Puente, G.; Sedran, U. Appl Catal B: Environ 1998, 19, 305.

20. Ghanbari-Siakhalu, A.; Garforth, A.; Cundy, C. S.; Dwyer, J. J Mater Chem 2001, 11, 569.
21. Marcilla, A.; Gomez, A.; Reyes-Labrta, A.; Giner, A. Polym Degrad Stab 2003, 80, 233.
22. Gobin, K.; Monos, G. Polym Degrad Stab 2004, 86, 225.
23. Puente, G.; Klocker, C.; Sedran, U. Appl Catal B: Environ 2002, 36, 279.
24. Salvador, C. C.; Avelino, C. Appl Catal B: Environ 2000, 25, 151.
25. Ali, S.; Garforth, A.; Harris, D. H.; Rawlence, D. J.; Uemichi, Y. Catal Today 2002, 75, 247.
26. Lin, Y. H.; Yang, M. H. J Mol Catal A: Chem 2001, 171, 143.
27. Lin, Y. H.; Yang, M. H. J Mol Catal A: Chem 2005, 231, 113.
28. Lin, Y. H.; Yang, M. H. Appl Catal B: Env 2007, 69, 145.
29. Lin, Y. H.; Yang, M. H. Appl Catal A: Gen 2007, 328, 132.
30. Beck, J. S.; Calabro, D. C.; Mccullen, S. B.; Pelrine, B. P.; Schmitt, K. D.; Vartuli, J. C. U.S. Pat. 5,145,816 (1992).
31. Lin, Y. H.; Yang, M. H. Thermochim Acta 2008, 471, 52.